

Naval Research Laboratory

Washington, DC 20375-5000



(2)

NRL Memorandum Report 6752

AD-A229 758

The Impact of the Three-Wave Instability on the Spiral Line Induction Accelerator

J. KRALL AND C. M. TANG

*Beam Physics Branch
Plasma Physics Division*

November 23, 1990

DTIC
SELECTED
DEC 11 1990
S B D
Go

REPORT DOCUMENTATION PAGE

Form Approved
OMB No. 0704-0188

Public reporting burden for this collection of information is estimated to average 1 hour per response, including the time for reviewing instructions, searching existing data sources, gathering and maintaining the data needed, and completing and reviewing the collection of information. Send comments regarding this burden estimate or any other aspect of this collection of information, including suggestions for reducing this burden, to Washington Headquarters Services, Directorate for Information Operations and Reports, 1215 Jefferson Davis Highway, Suite 1204, Arlington, VA 22202-4302, and to the Office of Management and Budget, Paperwork Reduction Project (0704-0188), Washington, DC 20503.

1. AGENCY USE ONLY (Leave blank)			2. REPORT DATE 1990 November 23	3. REPORT TYPE AND DATES COVERED
4. TITLE AND SUBTITLE The Impact of the Three-Wave Instability on the Spiral Line Induction Accelerator			5. FUNDING NUMBERS ARPA Order # 4395, A86 JO # 47-3593-00	
6. AUTHOR(S) J. Krall and C. M. Tang				
7. PERFORMING ORGANIZATION NAME(S) AND ADDRESS(ES) Naval Research Laboratory Code 4790 Washington, DC 20375-5000			8. PERFORMING ORGANIZATION REPORT NUMBER NRL Memorandum Report 6752	
9. SPONSORING/MONITORING AGENCY NAME(S) AND ADDRESS(ES) DARPA Arlington, VA 22209			10. SPONSORING/MONITORING AGENCY REPORT NUMBER NSWC Silver Spring, MD 20903-5000	
11. SUPPLEMENTARY NOTES				
12a. DISTRIBUTION/AVAILABILITY STATEMENT Approved for public release; distribution unlimited.			12b. DISTRIBUTION CODE	
13. ABSTRACT (Maximum 200 words) The solenoidal and helical quadrupole magnetic fields that are used to transport the high-current beam in the spiral line induction accelerator may admit instabilities such as the electromagnetic three-wave instability. Previous studies have shown that stability is easily maintained for energies up to = 40 MeV. We find that three-wave growth rates for energies exceeding 40 MeV can be $\leq 10^{-3}$ cm $^{-4}$. Strategies are outlined for stabilizing or further reducing growth rates. These are 1) cyclotron detuning, where the instability is detuned by varying the axial magnetic field, 2) damping the instability through the use of a low-Q beam pipe, where "low-Q" can include Q as high as 40,000 and 3) use of discrete quadrupole focusing, which allows the instability to be detuned by varying the quadrupole wavenumber. The effectiveness of de-Qing and cyclotron detuning is discussed for the various instability regimes.				
14. SUBJECT TERMS High current Accelerator			15. NUMBER OF PAGES 16	
17. SECURITY CLASSIFICATION OF REPORT UNCLASSIFIED			18. SECURITY CLASSIFICATION OF THIS PAGE UNCLASSIFIED	19. SECURITY CLASSIFICATION OF ABSTRACT UNCLASSIFIED
20. LIMITATION OF ABSTRACT SAR				

CONTENTS

I. INTRODUCTION	1
II. DETUNING IN THREE-WAVE UNSTABLE REGIME II	3
III. DAMPING VIA LOW Q	5
IV. DISCREET QUADRUPOLE FOCUSING	6
V. CONCLUSIONS	8
ACKNOWLEDGMENTS	8
REFERENCES	9

Accession For	
NTIS GRA&I	<input checked="" type="checkbox"/>
DATA TAB	<input type="checkbox"/>
Unpublished	<input type="checkbox"/>
Journal Article	<input type="checkbox"/>
By _____	
Distribution/	
Sensitivity Codes	
1. All and/or	
2. _____	
3. _____	
4. _____	
5. _____	
6. _____	
7. _____	
8. _____	
9. _____	
10. _____	
11. _____	
12. _____	
13. _____	
14. _____	
15. _____	
16. _____	
17. _____	
18. _____	
19. _____	
20. _____	
21. _____	
22. _____	
23. _____	
24. _____	
25. _____	
26. _____	
27. _____	
28. _____	
29. _____	
30. _____	
31. _____	
32. _____	
33. _____	
34. _____	
35. _____	
36. _____	
37. _____	
38. _____	
39. _____	
40. _____	
41. _____	
42. _____	
43. _____	
44. _____	
45. _____	
46. _____	
47. _____	
48. _____	
49. _____	
50. _____	
51. _____	
52. _____	
53. _____	
54. _____	
55. _____	
56. _____	
57. _____	
58. _____	
59. _____	
60. _____	
61. _____	
62. _____	
63. _____	
64. _____	
65. _____	
66. _____	
67. _____	
68. _____	
69. _____	
70. _____	
71. _____	
72. _____	
73. _____	
74. _____	
75. _____	
76. _____	
77. _____	
78. _____	
79. _____	
80. _____	
81. _____	
82. _____	
83. _____	
84. _____	
85. _____	
86. _____	
87. _____	
88. _____	
89. _____	
90. _____	
91. _____	
92. _____	
93. _____	
94. _____	
95. _____	
96. _____	
97. _____	
98. _____	
99. _____	
100. _____	
101. _____	
102. _____	
103. _____	
104. _____	
105. _____	
106. _____	
107. _____	
108. _____	
109. _____	
110. _____	
111. _____	
112. _____	
113. _____	
114. _____	
115. _____	
116. _____	
117. _____	
118. _____	
119. _____	
120. _____	
121. _____	
122. _____	
123. _____	
124. _____	
125. _____	
126. _____	
127. _____	
128. _____	
129. _____	
130. _____	
131. _____	
132. _____	
133. _____	
134. _____	
135. _____	
136. _____	
137. _____	
138. _____	
139. _____	
140. _____	
141. _____	
142. _____	
143. _____	
144. _____	
145. _____	
146. _____	
147. _____	
148. _____	
149. _____	
150. _____	
151. _____	
152. _____	
153. _____	
154. _____	
155. _____	
156. _____	
157. _____	
158. _____	
159. _____	
160. _____	
161. _____	
162. _____	
163. _____	
164. _____	
165. _____	
166. _____	
167. _____	
168. _____	
169. _____	
170. _____	
171. _____	
172. _____	
173. _____	
174. _____	
175. _____	
176. _____	
177. _____	
178. _____	
179. _____	
180. _____	
181. _____	
182. _____	
183. _____	
184. _____	
185. _____	
186. _____	
187. _____	
188. _____	
189. _____	
190. _____	
191. _____	
192. _____	
193. _____	
194. _____	
195. _____	
196. _____	
197. _____	
198. _____	
199. _____	
200. _____	
201. _____	
202. _____	
203. _____	
204. _____	
205. _____	
206. _____	
207. _____	
208. _____	
209. _____	
210. _____	
211. _____	
212. _____	
213. _____	
214. _____	
215. _____	
216. _____	
217. _____	
218. _____	
219. _____	
220. _____	
221. _____	
222. _____	
223. _____	
224. _____	
225. _____	
226. _____	
227. _____	
228. _____	
229. _____	
230. _____	
231. _____	
232. _____	
233. _____	
234. _____	
235. _____	
236. _____	
237. _____	
238. _____	
239. _____	
240. _____	
241. _____	
242. _____	
243. _____	
244. _____	
245. _____	
246. _____	
247. _____	
248. _____	
249. _____	
250. _____	
251. _____	
252. _____	
253. _____	
254. _____	
255. _____	
256. _____	
257. _____	
258. _____	
259. _____	
260. _____	
261. _____	
262. _____	
263. _____	
264. _____	
265. _____	
266. _____	
267. _____	
268. _____	
269. _____	
270. _____	
271. _____	
272. _____	
273. _____	
274. _____	
275. _____	
276. _____	
277. _____	
278. _____	
279. _____	
280. _____	
281. _____	
282. _____	
283. _____	
284. _____	
285. _____	
286. _____	
287. _____	
288. _____	
289. _____	
290. _____	
291. _____	
292. _____	
293. _____	
294. _____	
295. _____	
296. _____	
297. _____	
298. _____	
299. _____	
300. _____	
301. _____	
302. _____	
303. _____	
304. _____	
305. _____	
306. _____	
307. _____	
308. _____	
309. _____	
310. _____	
311. _____	
312. _____	
313. _____	
314. _____	
315. _____	
316. _____	
317. _____	
318. _____	
319. _____	
320. _____	
321. _____	
322. _____	
323. _____	
324. _____	
325. _____	
326. _____	
327. _____	
328. _____	
329. _____	
330. _____	
331. _____	
332. _____	
333. _____	
334. _____	
335. _____	
336. _____	
337. _____	
338. _____	
339. _____	
340. _____	
341. _____	
342. _____	
343. _____	
344. _____	
345. _____	
346. _____	
347. _____	
348. _____	
349. _____	
350. _____	
351. _____	
352. _____	
353. _____	
354. _____	
355. _____	
356. _____	
357. _____	
358. _____	
359. _____	
360. _____	
361. _____	
362. _____	
363. _____	
364. _____	
365. _____	
366. _____	
367. _____	
368. _____	
369. _____	
370. _____	
371. _____	
372. _____	
373. _____	
374. _____	
375. _____	
376. _____	
377. _____	
378. _____	
379. _____	
380. _____	
381. _____	
382. _____	
383. _____	
384. _____	
385. _____	
386. _____	
387. _____	
388. _____	
389. _____	
390. _____	
391. _____	
392. _____	
393. _____	
394. _____	
395. _____	
396. _____	
397. _____	
398. _____	
399. _____	
400. _____	
401. _____	
402. _____	
403. _____	
404. _____	
405. _____	
406. _____	
407. _____	
408. _____	
409. _____	
410. _____	
411. _____	
412. _____	
413. _____	
414. _____	
415. _____	
416. _____	
417. _____	
418. _____	
419. _____	
420. _____	
421. _____	
422. _____	
423. _____	
424. _____	
425. _____	
426. _____	
427. _____	
428. _____	
429. _____	
430. _____	
431. _____	
432. _____	
433. _____	
434. _____	
435. _____	
436. _____	
437. _____	
438. _____	
439. _____	
440. _____	
441. _____	
442. _____	
443. _____	
444. _____	
445. _____	
446. _____	
447. _____	
448. _____	
449. _____	
450. _____	
451. _____	
452. _____	
453. _____	
454. _____	
455. _____	
456. _____	
457. _____	
458. _____	
459. _____	
460. _____	
461. _____	
462. _____	
463. _____	
464. _____	
465. _____	
466. _____	
467. _____	
468. _____	
469. _____	
470. _____	
471. _____	
472. _____	
473. _____	
474. _____	
475. _____	
476. _____	
477. _____	
478. _____	
479. _____	
480. _____	
481. _____	
482. _____	
483. _____	
484. _____	
485. _____	
486. _____	
487. _____	
488. _____	
489. _____	
490. _____	
491. _____	
492. _____	
493. _____	
494. _____	
495. _____	
496. _____	
497. _____	
498. _____	
499. _____	
500. _____	
501. _____	
502. _____	
503. _____	
504. _____	
505. _____	
506. _____	
507. _____	
508. _____	
509. _____	
510. _____	
511. _____	
512. _____	
513. _____	
514. _____	
515. _____	
516. _____	
517. _____	
518. _____	
519. _____	
520. _____	
521. _____	
522. _____	
523. _____	
524. _____	
525. _____	
526. _____	
527. _____	
528. _____	
529. _____	
530. _____	
531. _____	
532. _____	
533. _____	
534. _____	
535. _____	
536. _____	
537. _____	
538. _____	
539. _____	
540. _____	
541. _____	
542. _____	
543. _____	
544. _____	
545. _____	
546. _____	
547. _____	
548. _____	
549. _____	
550. _____	
551. _____	
552. _____	
553. _____	
554. _____	
555. _____	
556. _____	
557. _____	
558. _____	
559. _____	
560. _____	
561. _____	
562. _____	
563. _____	
564. _____	
565. _____	
566. _____	
567. _____	
568. _____	
569. _____	
570. _____	
571. _____	
572. _____	
573. _____	
574. _____	
575. _____	
576. _____	
577. _____	
578. _____	
579. _____	
580. _____	
581. _____	
582. _____	
583. _____	
584. _____	
585. _____	
586. _____	
587. _____	
588. _____	
589. _____	
590. _____	
591. _____	
592. _____	
593. _____	
594. _____	
595. _____	
596. _____	
597. _____	
598. _____	
599. _____	
600. _____	
601. _____	
602. _____	
603. _____	
604. _____	
605. _____	
606. _____	
607. _____	
608. _____	
609. _____	
610. _____	
611. _____	
612. _____	
613. _____	
614. _____	
615. _____	
616. _____	
617. _____	
618. _____	
619. _____	
620. _____	
621. _____	
622. _____	
623. _____	
624. _____	
625. _____	
626. _____	
627. _____	
628. _____	
629. _____	
630. _____	
631. _____	
632. _____	
633. _____	
634. _____	
635. _____	
636. _____	
637. _____	
638. _____	
639. _____	
640. _____	
641. _____	
642. _____	
643. _____	
644. _____	

THE IMPACT OF THE THREE-WAVE INSTABILITY ON THE SPIRAL LINE INDUCTION ACCELERATOR

I. INTRODUCTION

It has long been known that the strong focusing magnetic fields that are used to transport the high-current beam in the spiral line induction accelerator (SLIA)¹, may admit instabilities such as the three-wave instability.²⁻⁴ The SLIA includes solenoidal focusing in the straight sections and both solenoidal and stellarator (helical quadrupole) focusing in the curved sections. The stellarator fields are included to focus the space charge of the beam over a large energy bandwidth.

Recent results have shown that there are several stability regimes for the three-wave instability^{3,4} and that the SLIA proof-of-concept experiment (PoCE) can operate entirely in the stable regime. What has been less clear is the significance of the instability as the beam energy approaches 50 MeV. In the present paper we will address the difficulties associated with designing a three-wave stable SLIA with a peak beam energy of 50 MeV.

The three-wave instability is a resonant interaction between the beam centroid motion in the external magnetic fields and the TE_{11} mode of the beam pipe. The external fields include the axial field $B_z = B_0$ and the quadrupole field:

$$B_{qx} = -B_q k_q [x \sin(k_q z) - y \cos(k_q z)] \quad (1a)$$

$$B_{qy} = B_q k_q [x \cos(k_q z) + y \sin(k_q z)] , \quad (1b)$$

where $B_q k_q$ is the quadrupole gradient and k_q is the quadrupole wavenumber.

For $\gamma \gg 1$ the stability condition of Ref. 4 may be written as

$$K_0 > K_c \equiv \frac{k_q}{2} + \frac{1}{2} \left[\left(k_q - \frac{2\mu_{11}}{\gamma} \right)^2 + \frac{4\gamma k_q^2 K_q^2}{\mu_{11} (k_q - \mu_{11}/\gamma)} \right]^{1/2} , \quad (2)$$

where $\gamma = (1 - \beta^2)^{-1/2}$ is the usual relativistic factor for the beam, $K_0 = eB_0/\gamma\beta mc^2$ is the cyclotron wavenumber, $K_q = eB_q/\gamma\beta mc^2$, $\mu_{11} = 1.84/r_g$ is the cut-off frequency of the TE_{11} waveguide mode and r_g is the radius of the beam pipe. Note that for $K_q \ll (k_q \mu_{11}/4\gamma)^{1/2}$, Eq. (2) reduces to the stability condition of Ref 3. For example, with $\gamma = 90$, $k_q = 0.048 \text{ cm}^{-1}$ and $r_g = 3 \text{ cm}$, parameters typical of a high energy SLIA bend⁵, the stability condition of Ref. 3 is valid only for very small quadrupole gradients, $B_q k_q \ll 67 \text{ G/cm}$.

The stability condition Eq. (2) gives a lower limit on K_0 for given values of γ , k_q , $B_q k_q$ and r_g such that as the beam energy increases, greater values of $B_0 > 0$ are required for stability. With the complete set of stability conditions of Ref. 4, we obtain a stability diagram as shown in Fig. 1. Here, stable and unstable regions of (B_0, k_q) parameter space are delineated for given values of γ , $B_q k_q$, and r_g . In Fig. 1, $\gamma = 7$, $B_q k_q = 200 \text{ G/cm}$ and $r_g = 3 \text{ cm}$. Note first that the SLIA PoCE will operate in the stable region that appears for $B_0 > 0$ in Fig. 1. Note also that in our convention, $k_q > 0$, indicating a stellarator field with a right-handed pitch. For a left-handed stellarator field, $k_q < 0$, stable operation requires $B_0 < 0$.

The difficulty of satisfying Eq. (2) at high energy can be seen in the stability diagram, shown as Fig. 2, for $\gamma = 90$, $B_q k_q = 73.4 \text{ G/cm}$, and $r_g = 3 \text{ cm}$. Figure 2 shows that $B_0 > 8.5 \text{ kG}$ would be required for stability. This is confirmed by numerical solutions of the dispersion relation. Because such high values of B_0 may not be desirable and because three-wave growth rates fall as $\gamma^{-1/2}$, it may be favorable to operate in a mildly unstable regime at high energy. Typical mildly unstable parameters for a $\gamma = 90$ SLIA bend are shown in Table I. Our uncertainty as to how much growth is

tolerable suggests to us that we consider alternate strategies for reducing or eliminating growth in this regime.

In the present paper we discuss three such strategies. In section II we discuss detuning the instability by varying the axial guide field. Section II contains a discussion of the possibility of damping the instability through the use of a low-Q beam pipe. In section IV, we consider the possible use of a discrete alternating gradient quadrupole focussing system, also known as a FODO lattice. This opens up the possibility of detuning the instability by varying the quadrupole wavenumber. We summarize our results in section V.

II. DETUNING IN THREE-WAVE UNSTABLE REGIME II

Recent ELBA⁶ simulation results showed saturation of the instability in three-wave unstable regime II ($k_q/2 + 2K_q < K_o \leq K_c$). Unstable regime II corresponds to unstable region II of (B_o, k_q) parameter space as shown in Figs. 1 and 2. This saturation, which occurred without emittance growth or current loss, was the result of detuning.⁷ In this scenario, the beam loses energy to the TE_{11} waveguide mode and, at the same time, the parallel velocity of the beam is reduced as the transverse motion increases. Both of these effects increase the cyclotron wavenumber K_o such that the three-wave interaction is detuned. This detuning changes the frequency ω of the unstable mode. The transverse beam centroid motion, which has wavenumber ω/β_c , cannot respond promptly to this frequency shift with the result that the beam motion is damped.

Diagnostics of beam energy and axial and parallel velocity of the beam centroid from several ELBA runs that exhibited this saturation showed that both γ and β_z decreased by several percent as the instability grew.⁷ This

shifted the cyclotron wavenumber by $\approx 10\%$ from the point when the instability began to grow, which was taken to be one-third of the saturation distance, to the point of saturation. Solutions of the dispersion relation for those parameters showed that for a 10% change in either B_0 or γ such that K_0 increased by 10%, the unstable interaction point in (ω, k) space shifted so as to stabilize the previous region (in frequency space) of peak growth.

Analysis confirms that detuning in K_0 is effective in three-wave unstable regime II but has little or no effect in regime I ($K_c < k_q/2 - K_q$). To see this, we must reexamine the three-wave interaction. Here we consider unstable waveguide modes with $\omega > 0$, but the discussion carries easily to the $\omega < 0$ case. As one sweeps through the possible values of K_0 , the equation of the unstable beam mode in (ω, k) space in the $I_b \rightarrow 0, K_q \rightarrow 0$ limit changes.⁴ For $K_0 \leq 0$ (in unstable regime I), the equation of the beam mode is

$$k \approx \omega/c - k_q . \quad (3a)$$

For $0 < K_0 < k_q/2$ (also in regime I), the unstable mode is

$$k \approx \omega/c + K_0 - k_q . \quad (3b)$$

For $k_q/2 < K_0 < k_q$ (unstable regime II), the unstable mode is again given by

$$k \approx \omega/c + K_0 - k_q . \quad (3c)$$

For $K_0 > k_q$, the beam is stable in the $I_b \rightarrow 0, K_q \rightarrow 0$ limit.

We see that in unstable regime I, shifts in K_0 have little effect because the beam mode is either independent of K_0 or restricted to $K_0 < k_q/2$. In unstable regime II, detuning is possible and is observed.

These results suggest that it may be possible to operate with low growth rates in three-wave unstable regime II by employing cyclotron detuning. Here one periodically shifts the magnitude of the axial guide field to shift the instability from frequency to frequency, thus keeping transverse beam motion at any given frequency below significant levels. Numerical solutions of the dispersion relation show that the latter two cases of Table I can be detuned with shifts in B_o of $<10\%$.

A refinement of this detuning technique might include tuned stubs at the location of each change in the axial magnetic field value. In theory, these could be adjusted so as to reflect the low level TE_{11} mode at the point where the unstable frequency is shifted and a new mode begins to grow.

Note that Eqs. (3a-c) show that detuning the instability via changes in k_q , rather than K_o , may be possible. Results for alternating gradient quadrupole focusing systems, presented in section IV below, confirm this possibility. Fabricating a helical quadrupole magnet with a varying pitch length, however, is considered prohibitively expensive.

III. DAMPING VIA LOW Q

Because growth rates in the high energy regime are small, it may be possible to damp the instability by lowering the Q of the beam pipe. If we assume that the presence of damping does not change the nature of the instability, the three-wave interaction will be stabilized when

$$Q \leq \omega/2\Gamma_\infty \quad (4)$$

where ω is the frequency of the unstable waveguide mode and Γ_∞ is the growth rate from the linear dispersion relation with $Q = \infty$. Analytical results⁸ in which damping was added to the dispersion relation have verified Eq. (4).

For example, for the three parameter sets of Table I, the instability can be damped with the rather high Q values of 850, 3700 and 40,000 respectively.

Another example is the NRL modified betatron accelerator (MBA) in which the addition of strong focusing fields has aided the successful acceleration of a 1 kA electron beam through >38000 turns in the 100 cm major radius device to obtain 15 MeV.⁹ Typical MBA parameters are beam current $I_b = 1$ kA, $B_0 = -2$ kG, $B_q k_q = 20$ G/cm, $k_q = 0.06$ cm⁻¹ and $r_g = 15$ cm. As the beam is accelerated from 5 to 15 MeV, the growth rate varies from $\Gamma_\infty/c = 5.10 \times 10^{-4}$ cm⁻¹ to 3.04×10^{-4} cm⁻¹. Because the frequency of the unstable mode is insensitive to changes in the cyclotron wavenumber in this regime, the unstable frequency remains constant at $\omega/c = 0.16$ cm⁻¹ ($\omega = 4.8$ GHz). Here $Q \leq 150$ is required for stability. The MBA vacuum chamber has $Q \approx 150$. Three-wave stability was confirmed by radiation measurements using a broad-band antenna which showed radiation levels not exceeding those expected from single-particle emission.¹⁰

IV. DISCREET QUADRUPOLE FOCUSING

Discrete quadrupole focusing systems, also called FODO lattices, have stability properties that differ from helical quadrupole systems.¹¹ The focusing field for such a system may be approximated by

$$B_{qx} = -B_q k_q \cos(k_q z) y, \quad B_{qy} = -B_q k_q \cos(k_q z) x \quad (5)$$

where k_q is the FODO wavenumber, $B_q k_q$ is the FODO gradient, z is the axial coordinate and x and y are transverse coordinates. Note that the FODO lattice field has no preferred direction so that we expect $B_0 < 0$ to be equivalent to $B_0 > 0$. In fact, when the dispersion relation is solved and approximate stability boundaries are found¹¹, we obtain the stability diagram shown in Fig. 3. Here, $\gamma = 7$, $B_q k_q = 200$ G/cm and $r_g = 3$ cm.

It is clear from the stability diagram that the overall stability properties are not as favorable as in the helical quadrupole case. However, we find that for identical values of I_b , γ , $B_q k_q$ and k_q , peak growth rates are lower, typically by $2^{1/2}$, in the FODO configuration. Furthermore, the flexibility of the FODO system allows growth rates to be reduced via detuning in the FODO wavenumber k_q .

We find that the FODO wavenumber can be changed so as to shift the unstable mode from frequency to frequency. Also, this detuning mechanism is applicable to low axial magnetic fields ($0 \leq K_0 < k_q - 2K_q$) where cyclotron detuning is not effective. This is demonstrated in Fig. 4, which shows growth rate versus frequency for a FODO lattice with $B_0 = 0$, $B_q K_q = 200$ G/cm and two different values of $k_q = 0.4$ and 0.6 cm^{-1} . Here, $I_b = 10$ kA, $\gamma = 7$ and $r_g = 3$ cm. We see that the unstable range at $k_q = 0.6 \text{ cm}^{-1}$ is completely stabilized when the FODO wavenumber is shifted to $k_q = 0.4 \text{ cm}^{-1}$. As with the helical quadrupole case, detuning will be effective if the beam centroid wavenumber, $\omega/\beta c$, is changed often enough that significant transverse beam motion does not develop. This scenario may be complicated by the multiple unstable wavenumbers associated with the unstable frequency of the FODO system, making it difficult to detune the TE_{11} mode both in frequency and wavenumber as can be done in the helical quadrupole case. We note, however, that the importance of this is not well understood.

Furthermore, designing such a minimum-growth FODO system may be somewhat time and computing intensive. Note that the instability in this configuration has been verified using the ELBA simulation code.¹¹

V. CONCLUSIONS

Previous results have shown that three-wave stability in the SLIA is easily maintained for energies up to \approx 40 MeV. We find that growth rates for energies exceeding 40 MeV can be $\lesssim 10^{-3} \text{ cm}^{-1}$. It may be possible to determine whether growth rates of order 10^{-3} cm^{-1} are permissible over the last 2-3 bends of a 50 MeV SLIA via PoCE experiments. If such growth rates are not acceptable, we have outlined three strategies for stabilizing or reducing the three-wave interaction. These are 1) cyclotron detuning, wherein the instability is detuned over the length of a given bend by varying the axial magnetic field, 2) damping the instability through the use of a "low-Q" beam pipe and 3) discrete quadrupole focusing, for which it is feasible to detune the instability by varying the discrete quadrupole wavenumber over the length of the curve. We show that "low-Q" can include Q as high as 40,000. Note that de-Qing and cyclotron detuning are most effective in three-wave unstable regime II, where the interaction frequency is highest and is sensitive to the cyclotron wavenumber.

Acknowledgments

This work was supported by Defense Advanced Research Projects Agency, ARPA Order Number 4395, Amendment 86, monitored by Naval Surface Warfare Center. We are also grateful to D. Chernin, T. Hughes, P. Sprangle, G. Joyce and S. Putnam for many illuminating discussions.

References

1. A. Mondelli, D. Chernin, S. D. Putnam, L. Schlitt and V. Bailey, Proc. Sixth Intl. Conf. on High Power Particle Beams (Osaka, Japan), (1986); also V. Bailey, L. Schlitt, M. Tiefenback, S. Putnam, A. Mondelli, D. Chernin and J. Petillo, Proc. 1987 IEEE Part. Accel. Conf., 920 (1987).
2. T. P. Hughes and B. B. Godfrey, Phys. Fluids 29, 5 (1986).
3. D. Chernin and T. P. Hughes (private communication)
4. C. M. Tang, P. Sprangle, J. Krall, P. Serafim and F. Mako, Part. Accel. (in press).
5. S. Putnam (private communication).
6. G. Joyce, J. Krall and S. Slinker, Proc. of the Conf. on Computer Codes and the Linear Accel. Community, LANL Report LA-11857-C, 341 (1990).
7. J. Krall, C. M. Tang, G. Joyce and P. Sprangle, Phys. Fluids B (December, 1990).
8. T. Hughes (private communication).
9. C. A. Kapetanakos, L. K. Len, T. Smith, J. Golden, K. Smith, S. J. Marsh, D. Dialetis, J. Mathew, P. Loschialpo, J. H. Chang, Phys. Rev. Lett. 64, 2374 (1990).
10. C. A. Kapetanakos (private communication).
11. C. M. Tang, J. Krall, D. Chernin and T. Hughes, submitted to Phys. Rev. D.

Table I

<u>R_o (kG)</u>	<u>$B_q k_q$ (G/cm)</u>	<u>k_q (cm$^{-1}$)</u>	<u>ω/c (cm$^{-1}$)</u>	<u>Γ/c (cm$^{-1}$)</u>
-6.91	235.0	0.064	3.41	2.0×10^{-3}
7.10	73.4	0.048	11.23	1.5×10^{-3}
7.71	58.3	0.048	28.56	3.5×10^{-4}

Unstable growth rates and frequencies for typical SLIA achromat parameters⁵
with $\gamma = 90$, $I_b = 10$ kA, $r_g = 3$ cm and bend radius $R_o = 250$ cm.

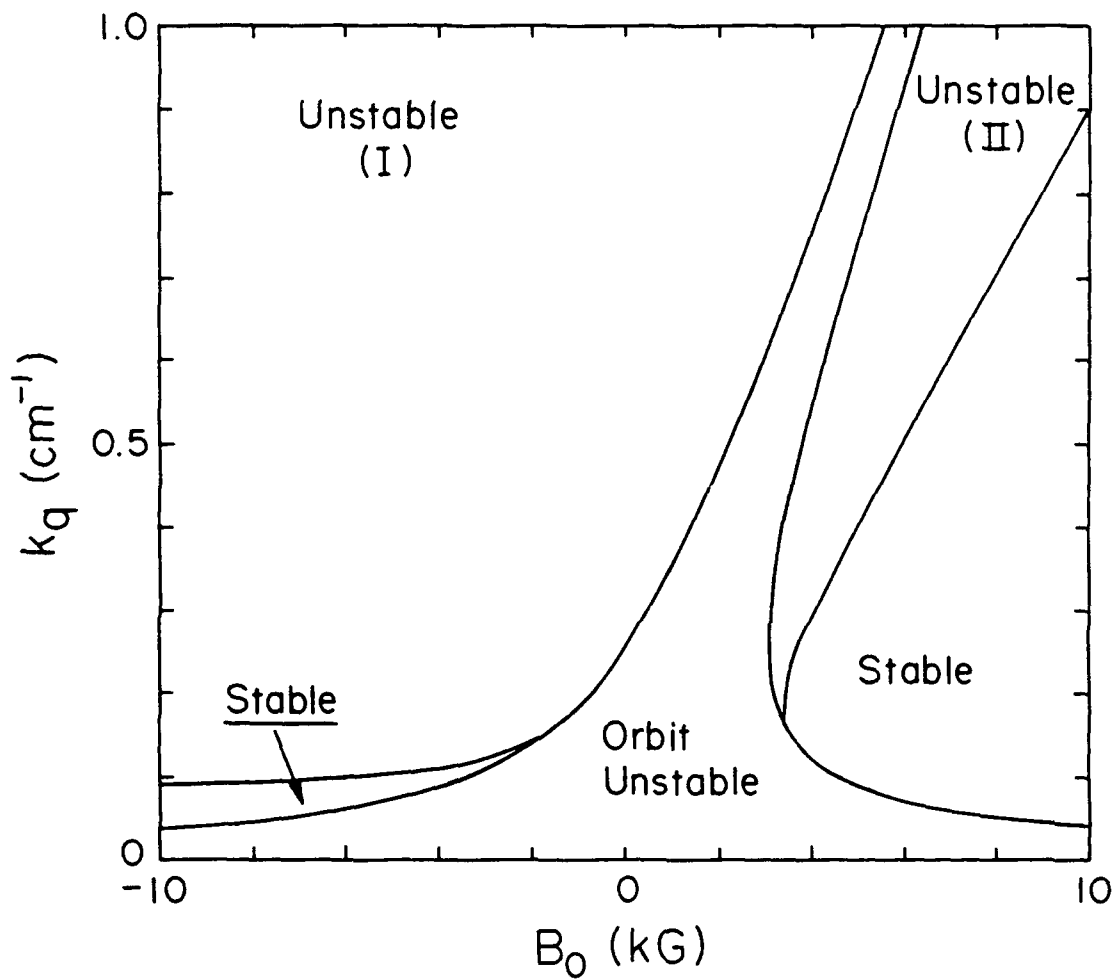


Fig. 1 — Stability diagram for beam energy $\gamma = 7$, quadrupole gradient $B_q k_q = 200$ G/cm and waveguide radius $r_g = 3$ cm

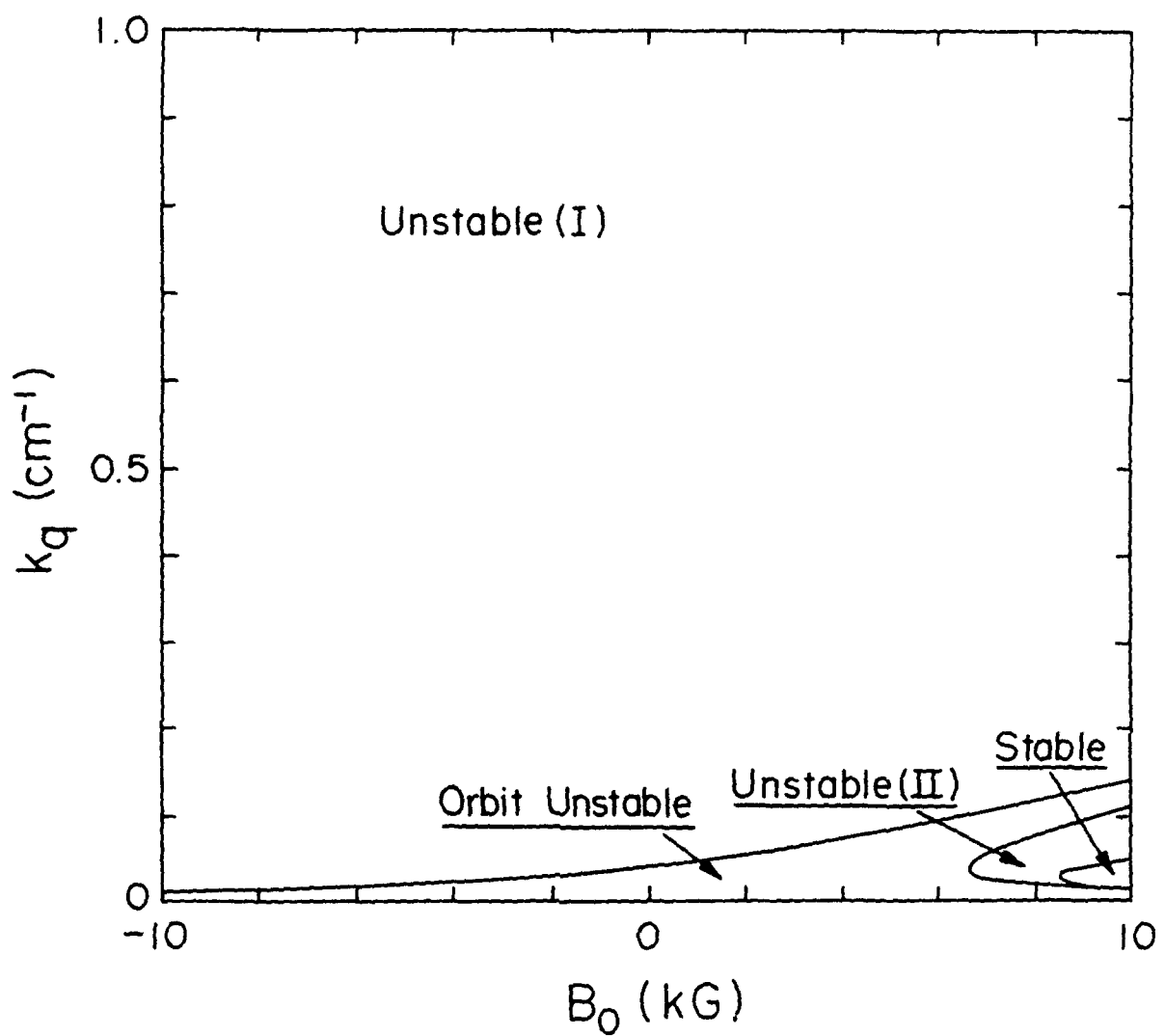


Fig. 2 — Stability diagram for beam energy $\gamma = 90$, quadrupole gradient $B_q k_q = 73.4$ G/cm and waveguide radius $r_g = 3$ cm

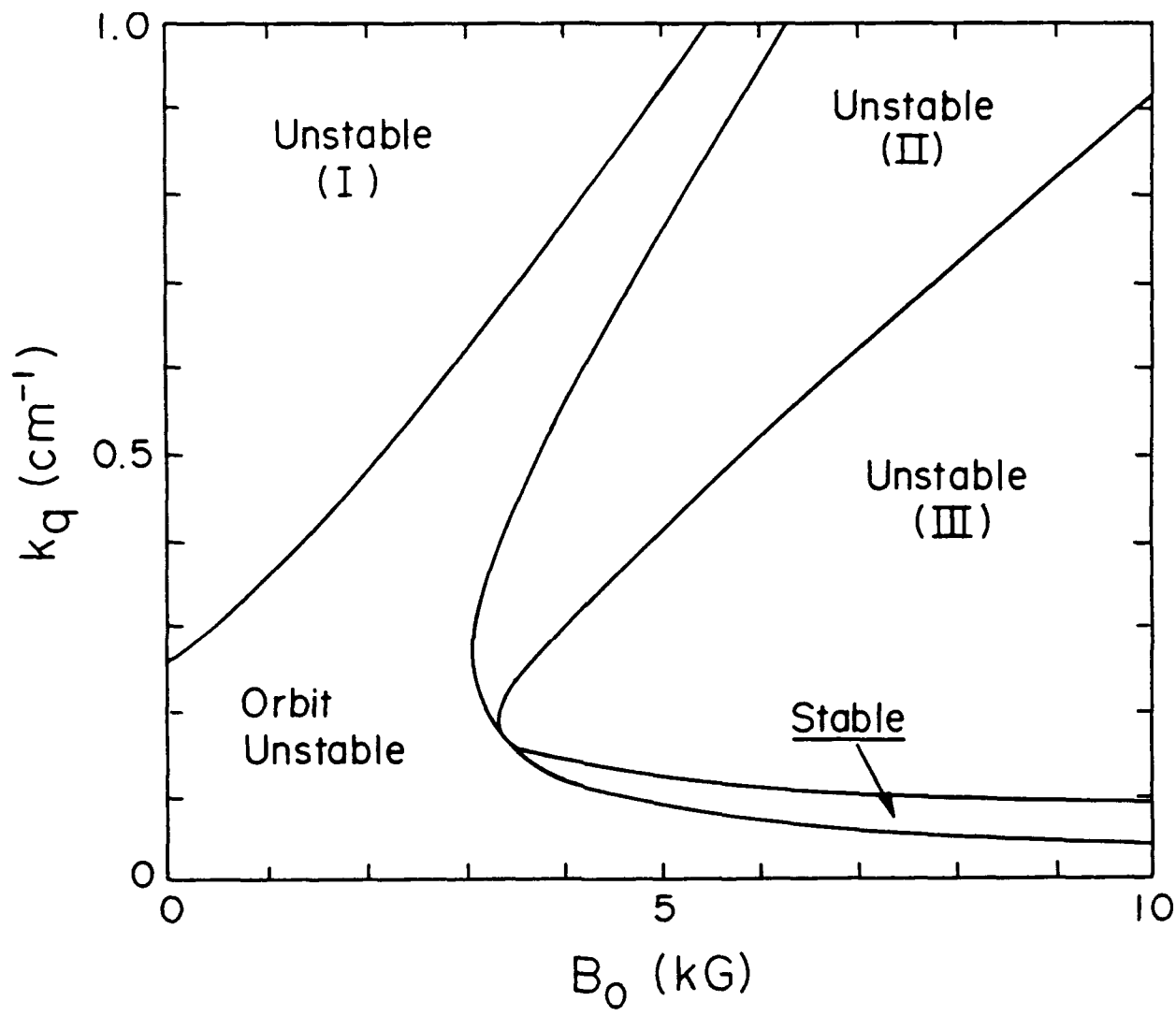


Fig. 3 — Stability diagram for a FODO lattice with beam energy $\gamma = 7$, quadrupole gradient $B_q k_q = 200 \text{ G/cm}$ and waveguide radius $r_g = 3 \text{ cm}$

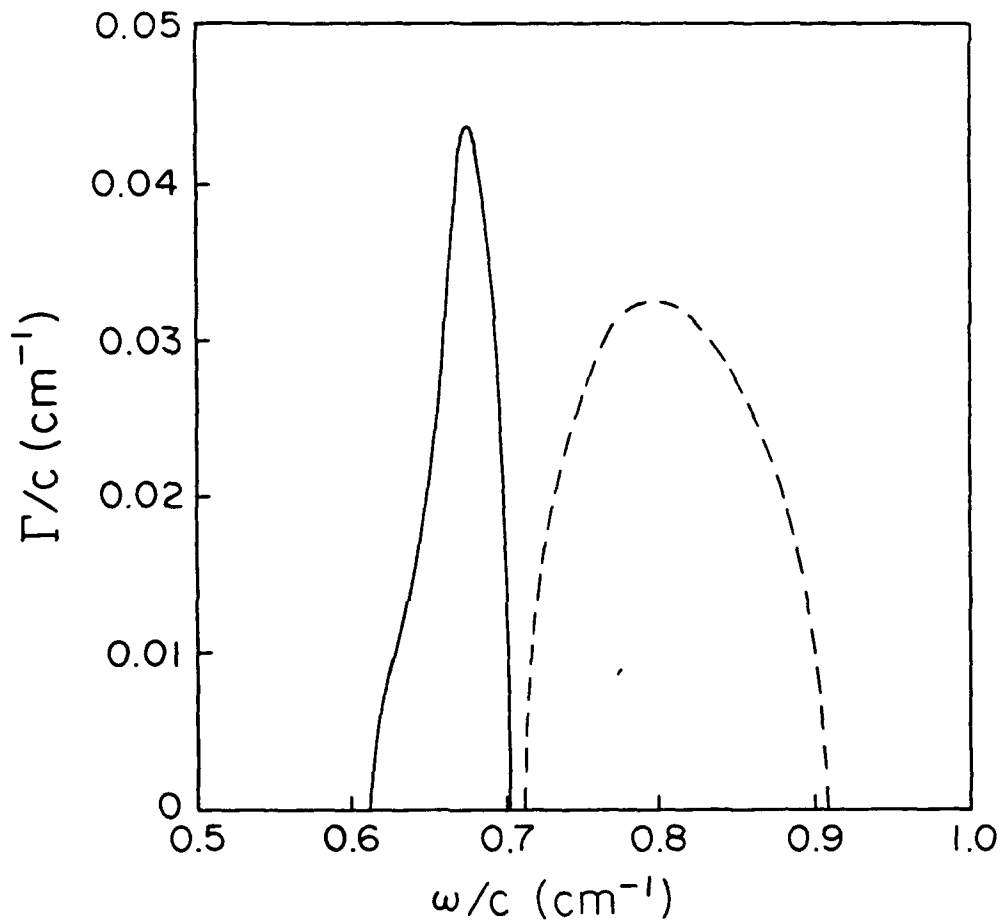


Fig. 4 — Growth rate Γ versus frequency ω for a discrete quadrupole focusing system with $B_0 = 0$, $B_q K_q = 200$ G/cm, $I_b = 10$ kA, $\gamma = 7$, $r_g = 3$ cm and two different values of $k_q = 0.6$ cm⁻¹ (solid) and 0.4 cm⁻¹ (dashed).